Analytical Biochemistry 443 (2013) 88–96

Contents lists available at ScienceDirect

Analytical Biochemistry

journal homepage: www.elsevier.com/locate/yabio

Profiling of lipid species by normal-phase liquid chromatography, nanoelectrospray ionization, and ion trap–orbitrap mass spectrometry

Elena Sokol [a,1], Reinaldo Almeida [a,1], Hans Kristian Hannibal-Bach [a], Dorota Kotowska [b], Johannes Vogt [c], Jan Baumgart [c], Karsten Kristiansen [b], Robert Nitsch [c], Jens Knudsen [a], Christer S. Ejsing [a,*]

[a] Department of Biochemistry and Molecular Biology, University of Southern Denmark, DK-5230 Odense, Denmark
[b] Department of Biology, University of Copenhagen, DK-2200 Copenhagen, Denmark
[c] Institute for Microscopic Anatomy and Neurobiology, Johannes Gutenberg University of Mainz, D-55128 Mainz, Germany

ARTICLE INFO

Article history:
Received 16 May 2013
Received in revised form 15 August 2013
Accepted 19 August 2013
Available online 29 August 2013

Keywords:
Lipidomics
Normal-phase LC
Nanoelectrospray ionization
Orbitrap mass spectrometry

ABSTRACT

Detailed analysis of lipid species can be challenging due to their structural diversity and wide concentration range in cells, tissues, and biofluids. To address these analytical challenges, we devised a reproducible, sensitive, and integrated lipidomics workflow based on normal-phase liquid chromatography–Fourier transform mass spectrometry (LC–FTMS) and LC–ITMS^2 (ion trap tandem mass spectrometry) for profiling and structural analysis of lipid species. The workflow uses a normal-phase LC system for efficient separation of apolar and polar lipid species combined with sensitive and specific analysis powered by a chip-based nanoelectrospray ion source and a hybrid ion trap–orbitrap mass spectrometer. The workflow was executed using a primary LC–FTMS survey routine for identification and profiling of lipid species based on high-mass accuracy and retention time followed by a targeted LC–ITMS^2 routine for characterizing the fatty acid moieties of identified lipid species. We benchmarked the performance of the workflow by characterizing the chromatographic properties of the LC–MS system for general lipid analysis. In addition, we demonstrate the efficacy of the workflow by reporting a study of low-abundant triacylglycerol and ceramide species in mouse brain cerebellum and 3T3-L1 adipocytes, respectively. The workflow described here is generic and can be extended for detailed lipid analysis of sample matrices having a wide range of lipid compositions.

Lipids comprise a diverse group of molecules that constitute membranes, store metabolic energy, and function as signaling molecules [1,2]. The complete repertoire of lipid molecules in a biological system is termed a lipidome. The dysregulation of lipid metabolism and lipid homeostasis is increasingly being assosiated with disorders such as type 2 diabetes, obesity, and neurodegenerative diseases [3]. To improve the understanding of lipid species and the lipidome in both physiological and pathophysiological processes warrants lipidomics routines supporting quantitative monitoring of lipid species on a global scale.

Various lipidomics technologies have been developed for comprehensive lipidome analysis [1,4–9]. These techniques are typically based on either direct infusion mass spectrometry (MS)[2] (also termed shotgun lipidomics) or liquid chromatography (LC)–MS. By shotgun lipidomics, lipid extracts are directly infused into the mass spectrometer, followed by high-resolution Fourier transform (FT) mass analysis and/or tandem mass analysis using specific precursor ion scans or neutral-loss scans to monitor lipid species [10–12]. Notably, shotgun lipidomics offers high analytical sensitivity and specificity and a wide dynamic quantification range of up to 4 orders of magnitude [13,14]. In comparison, LC–MS-based lipidomics routines feature an additional analytical dimension by chromatographic separation of lipid analytes. This separation can reduce potential ion suppression effects and facilitate unambiguous identification of isobaric lipid species that cannot be ascertained by shotgun lipidomics. The separation of lipid species is typically based on reverse-phase LC or occasionally normal-phase LC [15–19]. In reverse-phase LC, lipids are separated based primarily on the apolar properties of their fatty acid (FA) moieties. In comparison,

* Corresponding author. Fax: +45 6550 2467.
E-mail address: cse@bmb.sdu.dk (C.S. Ejsing).

[1] These authors contributed equally to this work.

[2] *Abbreviations used:* MS, mass spectrometry; LC, liquid chromatography; FT, Fourier transform; FA, fatty acid; IT, ion trap; FTMS, Fourier transform mass spectrometry; PI, phosphatidylinositol; ITMS, ion trap mass spectrometry; PVA–Sil, polyvinyl alcohol-functionalized silica; ITMS^2, ion trap tandem mass spectrometry; TAG, triacylglycerol; Cer, ceramide; HPLC, high-performance liquid chromatography; DMEM, Dulbecco's modified Eagle's medium; LCB, long-chain base; XIC, extracted ion chromatogram; DAG, diacylglycerol; PE, phosphatidylethanolamine; RT, retention time; HexCer, hexosylceramide; SHexCer, sulfatide; PG, phosphatidylglycerol; CL, cardiolipin; PC, phosphatidylcholine; SM, sphingomyelin; ACer, acyl-ceramide; CE, cholesteryl ester; LPC, lysophosphatidylcholine.

0003-2697/$ - see front matter © 2013 Elsevier Inc. All rights reserved.
http://dx.doi.org/10.1016/j.ab.2013.08.020

in normal-phase LC, lipid species are separated based primarily on the polarity of their head group structures. Because the differences in lipid class polarity are relatively larger than those of the FA moieties, the separation by lipid classes by normal-phase LC can be achieved in less time and with shorter columns [20]. Despite the utility of normal-phase LC-based lipid analysis, it remains a somewhat underused technique. This is due in part to the perception that chromatographic separations are difficult to reproduce and that the development of normal-phase resins has lagged behind their reverse-phase counterparts [21].

LC–MS-based lipidomics routines have been applied successfully for identification and quantification of lipid species using multiple reaction monitoring on triple quadrupole and quadrupole/linear ion trap (IT) instruments [17]. This type of targeted methodology can be highly sensitive but can equally be hampered by limited analytical specificity due to the low mass resolution and mass accuracy that can result in false-positive identification. In comparison, nontargeted methods based on high-resolution Fourier transform mass spectrometry (FTMS) analysis can reduce misidentification due to unsurpassed mass accuracy and afford direct identification of lipid species by sum composition nomenclature (e.g., phosphatidylinositol [PI] 38:4) [12]. The available instrumentation for FTMS analysis typically also supports identification of FA moieties of lipid species (e.g., PI 18:0–20:4) using ion trap multistage mass spectrometry (ITMS^n) or FTMS^n routines that provide either more sensitive or more specific analysis, respectively. These MS^n routines can be executed using nontargeted data-dependent acquisition technology for mapping abundant lipid analytes [12] or by using targeted multiplexed MS^n analysis for charting selected low-abundant lipid analytes. Notably, data-dependent acquisition using high-mass-resolution FTMS survey analysis ($\geqslant$100,000 full width at half maximum [FWHM]) and MS^2 analysis typically takes more than 2 s per cycle on hybrid linear IT–orbitrap instruments, which can hamper lipid profiling and structural analysis on LC time scales. Therefore, a workflow supporting high-resolution FTMS survey analysis and a complementary multiplexed MS^2 routine fast enough for lipid analysis on LC time scales could be beneficial.

Here we describe a novel normal-phase LC–MS-based workflow supporting profiling and structural characterization of lipid species. The workflow uses an LC system equipped with a polyvinyl alcohol-functionalized silica (PVA–Sil) column interfaced with a chip-based nanoelectrospray ion source and a hybrid IT–orbitrap mass spectrometer. The workflow entails a primary LC–FTMS survey routine for identification and profiling of lipid species based on high-mass accuracy and retention time and a secondary routine based on targeted LC–ITMS^2 (ion trap tandem mass spectrometry) analysis for identifying FA moieties of monitored lipid species. We benchmark the performance of the workflow by characterizing the chromatographic properties of the LC–MS system. Moreover, we demonstrate the efficacy of the workflow through a detailed study of low-abundant triacylglycerol (TAG) and ceramide (Cer) species in mouse brain cerebellum and 3T3-L1 adipocytes, respectively.

Materials and methods

Chemicals and lipid standards

Lipid standards and bovine liver extract were obtained from Avanti Polar Lipids (Alabaster, AL, USA). High-performance liquid chromatography (HPLC)-grade chloroform, methyl *tert*-butyl ether, and 2-propanol were obtained from Rathburn (Walkerburn, Scotland). HPLC-grade methanol and *n*-hexane were obtained from Fisher Scientific (Hampton, NH, USA). Ammonium acetate (HPLC grade), ammonium formate (HPLC grade), isobutylmethylxanthine (BioUltra), dexamethasone (BioReagent), and insulin (BioXtra) were purchased from Sigma–Aldrich (St. Louis, MO, USA).

Isolation of mouse cerebellum

A C57Bl/6 mouse was euthanized by an intraperitoneal injection of an anesthetic at an overdose. Subsequently, the mouse was perfused intracardially with cold 155 mM ammonium acetate and the cerebellum was dissected. The cerebellum was immediately frozen on dry ice and stored at −80 °C until further processing. The animal experiment was conducted in accordance with national laws for the use of animals in research and was approved by the local ethical committee.

Cell culture

3T3-L1 preadipocytes were cultured in Dulbecco's modified Eagle's medium (DMEM, Invitrogen, Taastrup, Denmark) with 10% calf serum (Invitrogen) at humidified 37 °C in the presence of 10% CO_2. Medium was changed every second day. Undifferentiated cells were harvested at day 2 post-confluence, washed twice with ice-cold 155 mM ammonium acetate buffer, transferred to a 15-ml Falcon tube, frozen in dry ice, and stored at −80 °C until further processing. 3T3-L1 cells were also differentiated to adipocytes by the addition of 500 μM isobutylmethylxanthine, 1 μM dexamethasone, and 167 nM insulin. After 48 h, the culture medium was replaced with DMEM containing 10% calf serum and 167 nM insulin. After that, medium was replaced every second day by DMEM with 10% calf serum. Cells were harvested at day 8 post-confluence as described for the undifferentiated 3T3-L1 preadipocytes. 3T3-L1 preadipocytes and adipocytes were disrupted by glass bead lysis, and aliquots of each cell homogenate were subjected to lipid extraction as outlined below.

Lipid extraction

Lipids were extracted by two-step lipid extraction at 4 °C as described previously [13,22]. In short, 3T3-L1 cells and mouse cerebellum homogenates corresponding to 10 μg of total protein (determined using a BCA [bisinchoninic acid] Protein Assay Kit, Thermo Scientific, Waltham, MA, USA) were diluted with 155 mM ammonium acetate to a final volume of 200 μl. Samples were subsequently added 990 μl of chloroform/methanol (10:1, v/v) and vigorously mixed for 120 min at 1400 rpm on a ThermoMixer (Eppendorf, Hamburg, Germany). Samples were centrifuged for 2 min at 500 g to promote phase separation. The lower organic phase was collected, vacuum evaporated, and dissolved in 60 μl of chloroform/methanol (1:2, v/v) prior to LC–MS analysis. A yeast lipid extract was prepared as described previously [13].

Lipid analysis by normal-phase LC–MS

Chromatographic separation was performed on a YMC-Pack PVA–Sil column (5 μm, 12 nm, 150 × 1.0 mm i.d.) with a 10 × 1-mm inner diameter YMC PVA–Sil guard column (YMC Europe, Schermbeck, Germany). LC–MS was executed using a Dionex P680 LC system equipped with a FAMOS autosampler (LC Packings). Then 1 μl of lipid extract or mixture of lipid standards was injected in microliter pickup mode using 4 mM ammonium formate in *n*-hexane/2-propanol/methyl *tert*-butyl ether (0.2:1.2:1, v/v/v) as transport solvent. The mobile phase solvents for binary gradient elution had the following compositions: 4 mM ammonium formate in 2-propanol/methyl *tert*-butyl ether (1.2:1, v/v, solvent A) and 4 mM ammonium formate in methanol (solvent B). The gradient elution program started with 100% A, increased to 100% B over 0.25 min, was maintained at 100% B for 10 min, increased to 100% A for 3 min, and was kept at 100% A until 20.5 min for column equilibration. The separation was performed at 37 °C using a flow rate of 50 μl/min.

The LC system was coupled to an LTQ Orbitrap mass spectrometer (Thermo Fisher Scientific, Bremen, Germany) via a TriVersa NanoMate ion source (Advion Biosciences, Ithaca, NY, USA) (Fig. 1). The LC flow rate of 50 µl/min was reduced using a low dead volume post-column split, resulting in an effective flow of 500 nl/min to the electrospray ionization (ESI) chip operated in positive or negative ion mode with a voltage of ±1.7 kV. In LC–FTMS survey mode, FTMS spectra were acquired either in positive ion mode (e.g., TAG analysis) or negative ion mode (e.g., Cer analysis) in the mass range of m/z 420 to 1500 with a target mass resolution of 100,000. This mode of analysis facilitated intensity profiling and identification of lipid species by sum composition based on accurate mass and retention time. The identified lipid species in a given sample extract were subsequently subjected to structural analysis for characterization of FA moieties by reanalyzing the extract using targeted LC–ITMS^2 mode operated in the same polarity as for the LC–FTMS survey analysis. In mode of operation, the precursor m/z values of identified lipid species were specified as separate multiplexed ITMS^2 scans. Up to 15 multiplexed ITMS^2 scans were specified in a single ITMS^2 method (i.e., for TAG analysis). All ITMS^2 experiments were performed using a collision energy of 35%, an activation Q of 0.25, and an ion isolation width of 2.0 amu. In addition, the targeted ITMS^2 routine featured an FTMS scan with target mass resolution of 30,000 to monitor ion spray performance throughout the LC–MS run. Detected lipid species were identified by ALEX (analysis of lipid experiments) software (manuscript in preparation). Lipid species and their fragment ions were identified by matching measured m/z of ions detected by FTMS and ITMS^2 to the calculated m/z stored in a lipid database.

Annotation of lipid species

Lipid species were annotated as described previously [11,13]. In short, lipid species were annotated either by sum composition when detected by FTMS analysis or by species composition when detected by ITMS^2 analysis. For example, when using sum composition Cer species were annotated as Cer (<lipid class>) <total number of C in the long-chain base (LCB) and FA moieties>:<total number of double bonds in the LCB and FA moieties>;<total number of OH groups in the LCB and FA moieties> (e.g., Cer 34:1;2), and when using species composition Cer species were annotated as Cer (<lipid class>) <total number of C in the LCB moiety>:<total number of double bonds in the LCB moiety>;<total number of OH groups in the LCB moiety>/<total number of C in the FA moiety>:<total number of double bonds in the FA moiety>;<total number of OH groups in the FA moiety> (e.g., Cer 18:1;2/16:0;0).

Results and discussion

Optimizing performance of normal-phase LC–MS system

The aim of this study was to develop a reproducible normal-phase LC–MS-based lipidomics routine. To this end, we combined an LC system equipped with a PVA–Sil column, a chip-based nano-electrospray ion source, and a high-resolution hybrid IT–orbitrap mass spectrometer (Fig. 1). In our initial efforts, we optimized each part of the LC–MS system. We observed that three factors were important for the performance of the LC–MS system: ion spray stability, choice of organic buffer, and gradient program. These factors are summarized below.

Ion spray stability

Previous applications of normal-phase LC using a PVA–Sil column have documented baseline separation of lipid classes using a ternary gradient program starting with a highly apolar solvent (e.g., heptane) followed by a solvent mixture of intermediate polarity (e.g., methyl *tert*-butyl ether/chloroform/isopropanol) and finally a more polar solvent (e.g., methanol) [19,23]. These solvents are typically added an ammonium salt to improve the separation of lipid analytes and to support stable ion spray for MS analysis. Our initial evaluation of ion spray performance, using an inbuilt spray sensing device on the ion source and extracted ion chromatograms (XICs), demonstrated stable and reproducible spray when using solvent mixtures of methyl *tert*-butyl ether/isopropanol (1.2:1, v/v) and methanol with ammonium acetate or formate at a final concentration of 1 to 25 mM (data not shown). Notably, we could not obtain stable ion spray when using the apolar solvents heptane or hexane. Consequently, we decided to omit the use of an initial highly apolar solvent and designed the LC program to use only a binary gradient composed of methyl *tert*-butyl ether/isopropanol (1.2:1, v/v, solvent A) followed by methanol (solvent B). By using this binary gradient, we sacrificed the capacity to baseline separate the apolar lipid classes TAG, diacylglycerol (DAG), and Cer, which coeluted early in the LC run (Fig. 2). Importantly, this loss of separation capacity did not interfere with the analytical specificity because the apolar lipid analytes can be distinguished based on high-resolution FTMS analysis and their distinct fragment ions and selective ionization properties in positive and negative ion modes. Moreover, using this gradient program, we achieved an analytical runtime of 20.5 min including column equilibration. We note that Sommer and coworkers [19] inserted a post-column feed (2.5 µl/min) to stabilize ion spray in the presence of heptane and thereby could achieve baseline separation of apolar lipid

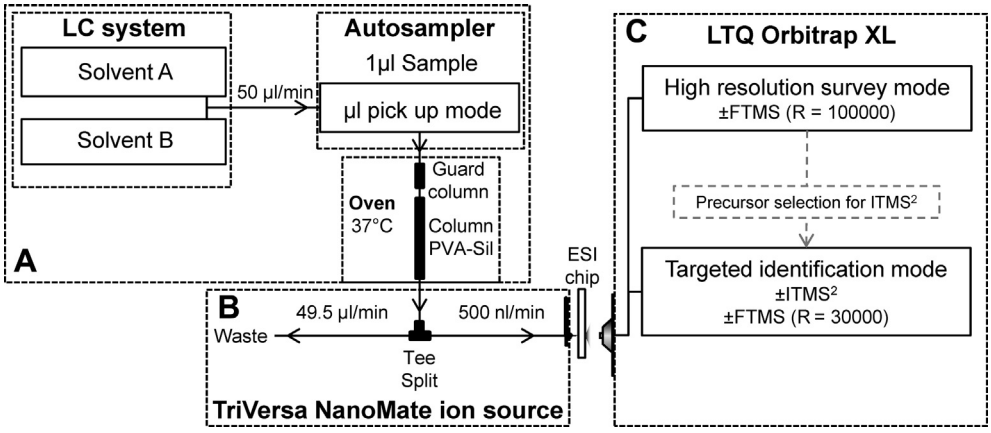

Fig.1. Schematic representation of the LC–MS system. (A) LC system including the autosampler and column. (B) TriVersa NanoMate ion source featuring a low-volume post-column split. (C) LTQ Orbitrap XL instrument operated in either high-resolution FTMS survey mode or targeted ITMS^2 identification mode.

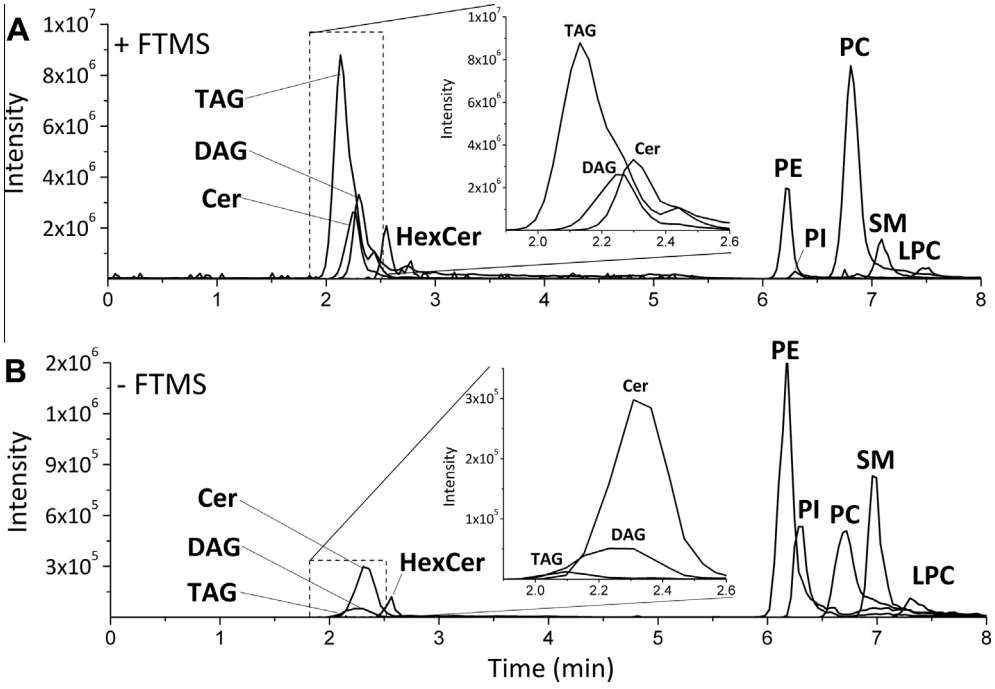

Fig.2. Chromatographic performance of the normal-phase LC system. XICs of selected TAG, DAG, Cer, HexCer, PC, PI, PE, SM, and LPC species in a lipid extract from bovine liver are shown. (A) Positive ion FTMS. TAG, DAG, and PI species were detected as $[M+NH_4]^+$, and other species were detected as $[M+H]^+$. (B) Negative ion FTMS. TAG, DAG, Cer, HexCer, PC, SM, and LPC were detected as $[M+HCOO]^-$, and other species were detected as $[M-H]^-$). Note that TAG species display poor ionization efficiency in the negative ion mode, which facilitates the detection of Cer and DAG species in this ion mode. TAG, triacylglycerol; DAG, diacylglycerol; Cer, ceramide; HexCer, hexosylceramide; PC, phosphatidylcholine; PI, phosphatidylinositol; PE, phosphatidylethanolamine; SM, sphingomyelin; LPC, lysophosphatidylcholine.

classes. We considered making use of a post-column feed but judged this to be technically cumbersome given our low flow rate after the post-column split (500 nl/min).

Effect of organic buffers

We also tested the efficacy of different organic buffers in the solvent system. We achieved optimal sensitivity when using either ammonium formate or ammonium acetate. The inclusion of triethylamine/formic acid (1:1, mol/mol) compromised sensitivity but, interestingly, inverted the retention of phosphatidylethanolamine (PE) and PI compared with using the ammonium salts (data not shown). When using ammonium acetate for negative ion mode LC–MS analysis, we observed a relatively high abundance of Cer and DAG species carrying a formate adduct ($[M+HCOO]^-$) instead

Table 1
Chromatographic properties of the normal-phase LC–MS system.

Lipid species	RT ± SD (min)	+FTMS		–FTMS		Preferential monitoring in ion mode
		m/z	Precursor	*m/z*	Precursor	
TAG 52:2[a]	2.13 ± 0.02	876.801	$[M+NH_4]^+$	903.766	$[M+HCOO]^-$	+
CE 18:1[a]	2.20 ± 0.02	668.634	$[M+NH_4]^+$	ND		+
ACer 18:1;2/17:0;0/18:1;0[c]	2.04 ± 0.02	816.780	$[M+H]^+$	860.771	$[M+HCOO]^-$	+
DAG 34:1[a]	2.20 ± 0.05	612.556	$[M+NH_4]^+$	639.521	$[M+HCOO]^-$	+/–
Cer 34:1;2[a]	2.30 ± 0.02	538.519	$[M+H]^+$	582.510	$[M+HCOO]^-$	+/–
HexCer 42:1;2[a]	2.42 ± 0.03	812.697	$[M+H]^+$	856.688	$[M+HCOO]^-$	+/–
GluCer 18:1;2/16:0;0[c]	3.17 ± 0.03	806.562	$[M+H]^+$	850.553	$[M+HCOO]^-$	+/–
SHexCer 18:1;2/12:0;0[c]	3.28 ± 0.05	724.466	$[M+H]^+$	724.466	$[M-H]^-$	–
PG 17:0/17:0[c]	4.23 ± 0.07	768.575	$[M+NH_4]^+$	749.534	$[M-H]^-$	–
CL 14:0/14:0/14:0/14:0[c]	5.81 ± 0.45	ND		1239.840	$[M-H]^-$	––
PE 38:4[a]	6.20 ± 0.02	768.554	$[M+H]^+$	766.539	$[M-H]^-$	+/–
PI 38:4[a]	6.30 ± 0.02	904.591	$[M+NH_4]^+$	885.550	$[M-H]^-$	–
IPC 44:0;4[b]	6.00 ± 0.02	ND		952.686	$[M-H]^-$	–
MIPC 44:0;4[b]	6.20 ± 0.01	ND		1114.739	$[M-H]^-$	–
PC 40:5[a]	6.80 ± 0.04	836.616	$[M+H]^+$	880.607	$[M+HCOO]^-$	+
SM 34:1;2[a]	7.10 ± 0.04	703.575	$[M+H]^+$	747.566	$[M+HCOO]^-$	+
LPC 16:0[a]	7.50 ± 0.05	496.340	$[M+H]^+$	540.330	$[M+HCOO]^-$	+

Note: TAG, triacylglycerol; CE, cholesteryl ester; Cer, ceramide; ACer, acyl-ceramide; DAG, diacylglycerol; HexCer, hexosylceramide; PE, phosphatidylethanolamine; GluCer, glucosylceramide; SHexCer, sulfatide; PG, phosphatidylglycerol, CL, cardiolipin; PI, phosphatidylinositol; PC, phosphatidylcholine; IPC, inositolphosphoceramide; MIPC, mannosyl-inositolphosphoceramide; SM, sphingomyelin; LPC, lysophosphatidylcholine; ND, not detected. Average retention time (RT) and standard deviation (SD) are based on at least six injections.

[a] Lipid species detected in a lipid extract from bovine liver.
[b] Lipid species detected in a lipid extract from yeast.
[c] Synthetic lipid standard.

Table 2
TAG species in mouse cerebellum.

Precursor FTMS *m/z*	TAG sum composition	ITMS^2 fragment *m/z*	Loss of FA	TAG species composition
822.755	TAG 48:1	577.5	14:0	TAG 14:0–16:0–18:1
		549.5	16:0	TAG 16:0–16:0–16:1
		551.5	16:1	
		523.5	18:1	
846.755	TAG 50:3	601.5	14:0	TAG 14:0–18:1–18:2
		573.5	16:0	TAG 16:0–16:0–18:3
		575.5	16:1	TAG 16:0–16:1–18:2
		547.5	18:1	
		549.5	18:2	
		551.5	18:3	
848.770	TAG 50:2	575.5	16:0	TAG 16:0–16:0–18:2
		577.5	16:1	TAG 16:0–16:1–18:1
		549.5	18:1	
		551.5	18:2	
		553.5	18:3	
850.786	TAG 50:1	577.5	16:0	TAG 16:0–16:0–18:1
		579.5	16:1	TAG 16:0–16:1–18:0
		549.5	18:0	
		551.5	18:1	
874.786	TAG 52:3	601.5	16:0	TAG 16:1–18:1–18:1
		603.5	16:1	TAG 16:0–18:1–18:2
		575.5	18:1	
		577.5	18:2	
876.801	TAG 52:2	603.5	16:0	TAG 16:0–18:0–18:2
		575.5	18:0	TAG 16:0–18:1–18:1
		577.5	18:1	
		579.5	18:2	
878.817	TAG 52:1	605.6	16:0	TAG 16:0–18:0–18:1
		577.5	18:0	
		579.5	18:1	
896.770	TAG 54:6	623.5	16:0	TAG 16:0–16:0–22:6
		599.5	18:2	TAG 16:0–18:2–20:4
		577.5	20:5	
		551.5	22:6	
900.801	TAG 54:4	627.5	16:0	TAG 18:1–18:1–18:2
		599.5	18:0	TAG 18:0–18:2–18:2
		601.5	18:1	TAG 16:0–18:0–20:4
		579.5	20:4	
902.817	TAG 54:3	603.5	18:1	TAG 18:1/18:1/18:1
904.833	TAG 54:2	631.6	16:0	TAG 18:0–18:1–18:1
		603.5	18:0	TAG 16:0–18:1–20:1
		605.6	18:1	
		577.5	20:1	
922.786	TAG 56:7	649.5	16:0	TAG 16:0–18:1–22:6
		623.5	18:1	
		577.5	22:6	
924.801	TAG 56:6	651.5	16:0	TAG 16:0–18:0–22:6
		623.5	18:0	TAG 16:0–18:1–22:5
		625.5	18:1	TAG 16:0–20:3–20:3
		601.5	20:3	TAG 18:1–18:1–20:4
		603.5	20:4	
		577.5	22:5	
		579.5	22:6	
968.770	TAG 60:12	623.5	22:6	TAG 16:0–22:6–22:6

Note. TAG species were identified by normal-phase LC–FTMS and LC–ITMS^2 analysis of a lipid extract of mouse cerebellum.

of the expected acetate adduct ($[M+CH_3COO]^-$). These lipid ions were initially falsely identified as odd-FA-chain-containing species. Comparison of negative and positive ion mode data and ITMS^2 analysis revealed that the LC-grade ammonium acetate was contaminated with formate. Negative ion mode time-of-flight mass analysis of the ammonium acetate confirmed the presence of a formate ion at *m/z* 45.00 (data not shown). Henceforth, we decided to use only ammonium formate as a buffer so as not to compromise analytical specificity.

Gradient program and chromatographic performance

To optimize the chromatographic performance of the normal-phase LC–MS system, we tested a variety of gradient programs. Inspired by previous applications [19,24], we initially evaluated the performance using a shallow gradient over several minutes starting from 100% 4 mM ammonium formate in methyl *tert*-butyl ether/2-propanol (60:40, v/v) to 100% 4 mM ammonium formate in methanol. We observed significant peak broadening of PE and PI species (data not shown). In an attempt to minimize peak

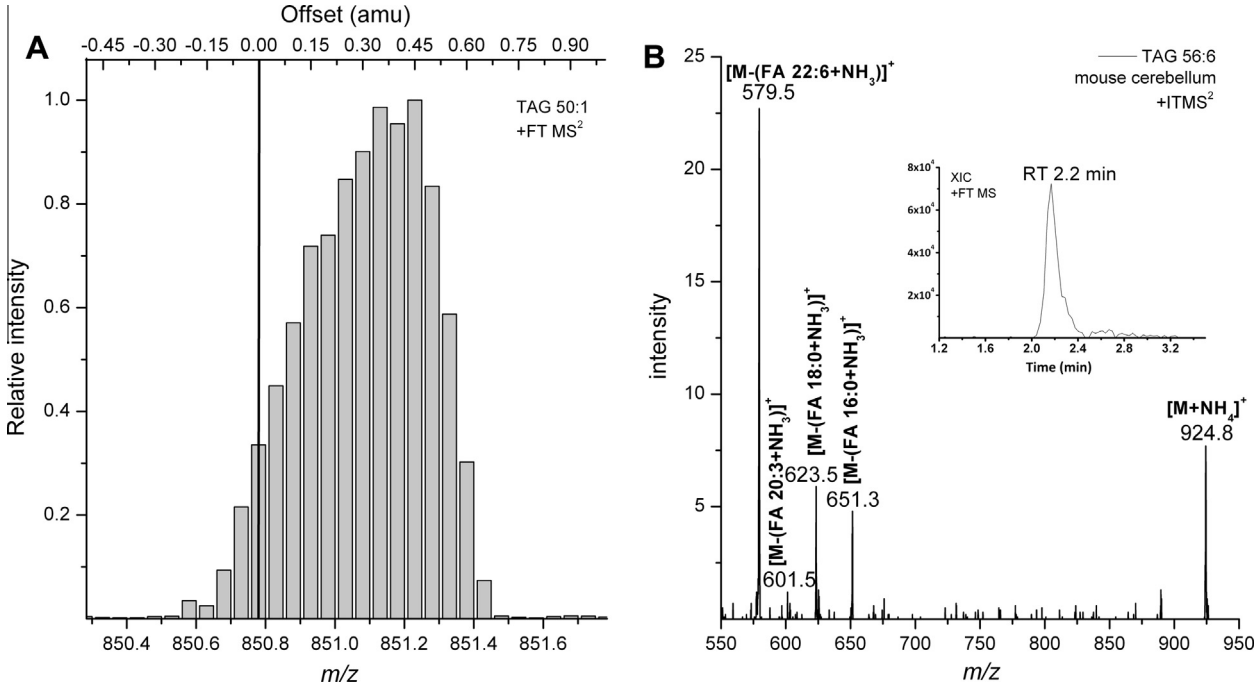

Fig.3. Normal-phase LC–MS analysis of TAG species in mouse cerebellum. (A) XIC of fragment ion m/z 551.503 ([TAG 50:1–(FA 18:1+NH_3)]$^+$) as function of selected precursor ion m/z. FTMS^2 spectra were recorded by stepping the ion trap target m/z by 0.05 amu steps over the m/z range [849.8;851.8]. The collision energy was 35%, and the precursor ion isolation width was 2.0 amu. The optimal intensity of TAG-derived fragment ions was obtained when a mass offset of 0.40 amu was added to the TAG precursor m/z selected for ITMS^2 analysis. The calculated m/z of the precursor ion [TAG 50:1+NH_4]$^+$ is denoted with a vertical line. (B) ITMS^2 spectrum of m/z 924.8+0.4 corresponding to [TAG 56:6+NH_4]$^+$. The TAG species undergo characteristic neutral loss of attached FA moieties that pinpoint the presence of four species: TAG 16:0–18:0–22:6, TAG 16:0–18:1–22:5, TAG 16:0–20:3–20:3, and TAG 18:1–18:1–20:4 (see Table 1). Inset: XIC of m/z 924.801 corresponding to [TAG 56:6+NH_4]$^+$ detected in a lipid extract of mouse cerebellum.

broadening, we tested the performance of a rapid gradient changing from 100% 4 mM ammonium formate in methyl *tert*-butyl ether/2-propanol (60:40, v/v) to 100% 4 mM ammonium formate in methanol in 15 s. This gradient program produced the best chromatographic peak resolution for all monitored lipid classes (Fig. 2).

Using the optimized LC conditions, we were able to separate apolar lipid classes from polar lipid classes with excellent run-to-run reproducibility (Table 1). Apolar TAG, DAG, and Cer species coeluted at the beginning of the LC run (retention time [RT] ~ 2.2 min), followed by hexosylceramide (HexCer, RT ~ 2.4–3.2 min, depending on the FA moiety), sulfatide (SHexCer, RT ~ 3.3 min), phosphatidylglycerol (PG, RT ~ 4.2 min), cardiolipin (CL, RT ~ 5.8 min), and eventually more polar PI, phosphatidylcholine (PC), PE, and sphingomyelin (SM) species after 6 min (Fig. 2 and Table 1). In addition, we observed that apolar acyl-ceramide (ACer) and cholesteryl ester (CE) coeluted with TAG, DAG, and Cer species. Moreover, we found that the LC–MS system supported analysis of yeast sphingolipids inositolphosphoceramide and mannosyl-inositolphosphoceramide, which eluted after 6 min (Table 1). We note that the LC–MS system did not afford monitoring of phosphatidic acid and phosphatidylserine species.

Ionization properties of lipid classes

Positive ion mode analysis demonstrated that the majority of lipids were detected as $[M+H]^+$ adduct ions except for TAG, DAG, CE, PG, and PI species, which were detected as $[M+NH_4]^+$ ions (Table 1). We note that a fraction of Cer species were detected as $[M+H-H_2O]^+$ due to in-source fragmentation. Negative ion mode analysis showed that TAG, DAG, Cer, PC, lysophosphatidylcholine (LPC), and SM species were detected as $[M+HCOO]^-$ adduct ions, whereas the majority of other lipids were detected as deprotonated $[M-H]^-$ ions. We note that Cer species were detected primarily as formate adduct ions and, to a lesser extent, as deprotonated ions. Comparison of the relative ionization efficiency showed that TAG, PC, LPC, and SM species ionized preferentially in positive ion mode, whereas PE and PI species ionized preferentially in negative ion mode. Cer and DAG species showed similar ionization efficiency in both positive and negative ion modes. Based on the differential ionization efficiency of TAG in positive and negative ion modes, we decided to apply the LC–MS system for (i) profiling of low-abundant TAG species in mouse cerebellum using positive ion mode analysis and (ii) profiling of low-abundant Cer species in 3T3-L1 adipocytes by negative ion mode analysis. To this end, we designed a workflow using a primary LC–FTMS survey routine for profiling and identification of lipid species (by sum composition) followed by secondary analysis using a targeted LC–ITMS^2 routine for identification of the FA moieties of identified lipid species.

Molecular profiling of low-abundant TAG species in brain

A preliminary shotgun lipidomics analysis indicated that TAG species constitute less than 0.1 mol% of the mouse cerebellum lipidome (data not shown). The LC–FTMS survey analysis of the same lipid extract executed in positive ion mode allowed identification of 15 TAG species (Table 2), with TAG 50:0, TAG 50:1, TAG 54:6, TAG 56:6, and TAG 56:7 being the most abundant. The 15 species were selected for targeted LC–ITMS^2 analysis to map the FA moieties of the TAG species; that is, the method featured 15 multiplexed ITMS^2 scans with m/z values corresponding to the identified TAG species. The fragmentation of TAG produces neutral loss of the FA moieties attached to the *sn*-1, *sn*-2, and *sn*-3 positions of the glycerol backbone, which in turn enables identification of their length and number of double bonds [25–27]. Importantly, prior to the LC–ITMS^2 analysis, we had evaluated various instrumental

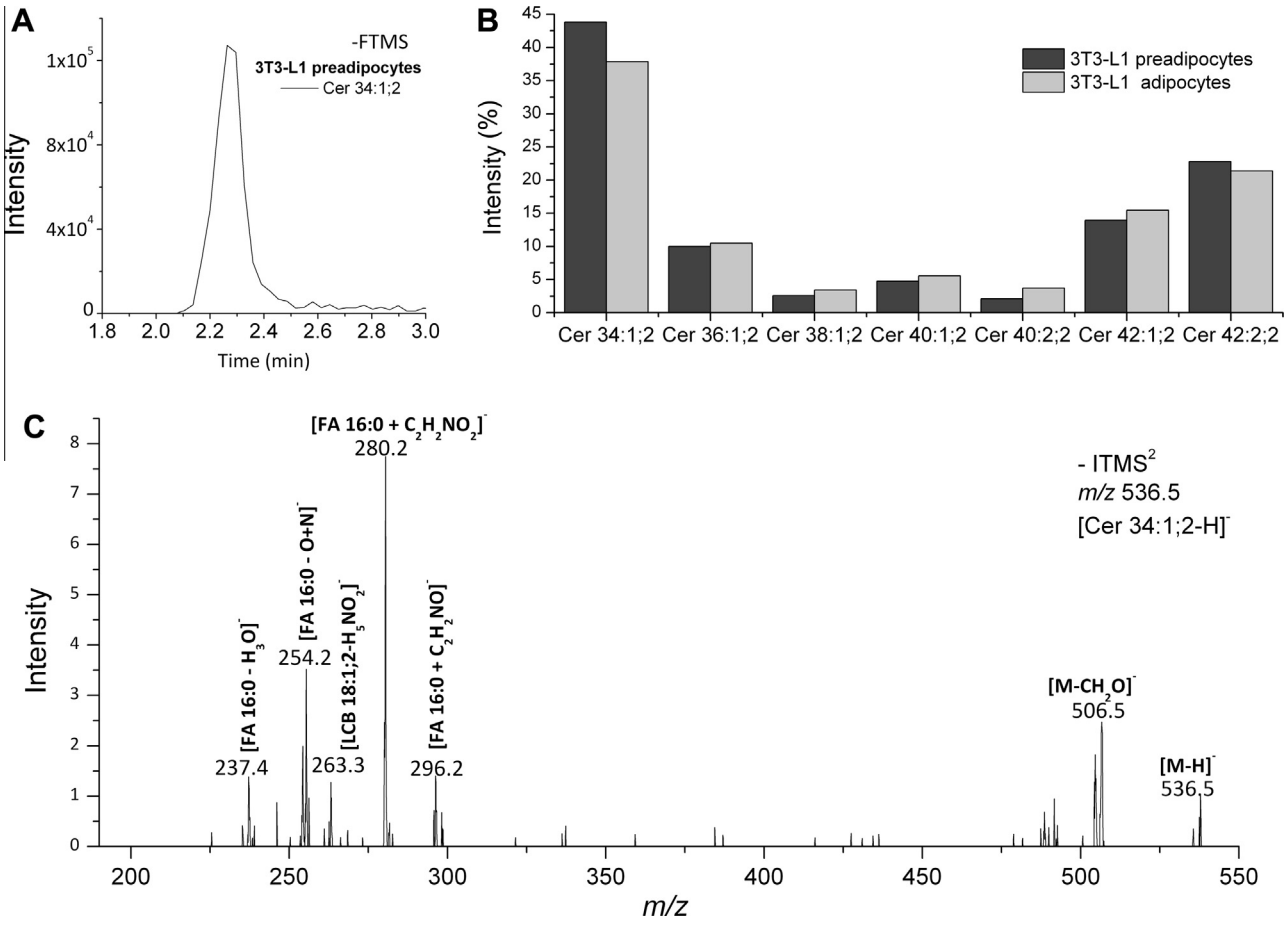

Fig.4. Normal-phase LC–FTMS and LC–ITMS^2 analysis of Cer species in 3T3-L1 preadipocytes and adipocytes. (A) XIC of *m/z* 582.519 corresponding to $[Cer\ 34:1;2+HCOO]^-$ monitored by negative ion mode FTMS. (B) Profile of Cer species in 3T3-L1 preadipocytes and adipocytes determined by LC–FTMS analysis. The intensity percentage of a given Cer species was calculated by normalizing its intensity to the sum of intensities of monitored Cer species. (C) ITMS^2 analysis of *m/z* 536.5 corresponding to Cer 18:1;2/16:0;0 (34:1;2) ($[M-H]^-$). Fragment ions are annotated according to structural attributes of the LCB and FA moiety. Note that Cer species are detected as formate adducts by FTMS and that ITMS^2 analysis uses the deprotonated precursor ion for isolation and fragmentation (see discussion in text).

Table 3
Cer species identified by LC–FTMS and LC–ITMS^2 analysis of lipid extracts from 3T3-L1 cell preadipocytes and adipocytes.

FTMS *m/z* $[M+HCOO]^-$	Sum composition	ITMS^2 *m/z* $[M-H]^-$	$[LCB-H_5NO_2]^-$ *m/z*	$[FA+C_2H_2NO_2]^-$ *m/z*	Species composition	Species composition[a]
582.510	Cer 34:1;2	536.5	263.2	280.3	Cer 18:1;2/16:0;0	Cer d18:1/16:0
610.542	Cer 36:1;2	564.5	291.3	308.3	Cer 18:1;2/18:0;0	Cer d18:1/18:0
638.573	Cer 38:1;2	592.6	319.3	336.3	Cer 18:1;2/20:0;0	Cer d18:1/20:0
666.604	Cer 40:1;2	622.6	347.3	364.4	Cer 18:1;2/22:0;0	Cer d18:1/22:0
664.589	Cer 40:2;2	620.6	345.3	362.3	Cer 18:1;2/22:1;0	Cer d18:1/22:1
694.635	Cer 42:1;2	648.6	375.4	392.4	Cer 18:1;2/24:0;0	Cer d18:1/24:0
692.620	Cer 42:2;2	646.6	373.3	390.4	Cer 18:1;2/24:1;0	Cer d18:1/24:1

[a] Traditional nomenclature using letter code to report the number of OH groups in the LCB moiety.

settings for optimal detection of TAG-derived fragment ions. Surprisingly, we observed that optimal detection of TAG-derived fragment ions required a systematic offset of the precursor *m/z* by 0.35 to 0.45 amu when an ion isolation width of 2.0 amu was applied (Fig. 3A). Hence, to obtain optimal conditions for LC–ITMS^2 analysis, we applied a precursor ion offset of 0.4 amu to all targeted TAG species. Notably, the systematic *m/z* offset was not required for optimal ITMS^2 analysis of PC, PE, and analytes used for tuning the instrumentation (data not shown). The LC–ITMS^2 analysis showed that the mouse cerebellum comprises TAG species with saturated, monounsaturated, and polyunsaturated FA moieties. For example, ITMS^2 analysis of $[TAG\ 56:6+NH_4]^+$ produced several fragment ions with *m/z* 651.5, 623.5, and 579.5 derived from the neutral loss of FA moieties 16:0, 18:0, and 22:6, respectively (Fig. 3B). This fragmentation pattern corresponds to the molecular species TAG 16:0–18:0–22:6. In summary, the LC–ITMS^2 analysis demonstrated that the molecular composition of TAG species in mouse cerebellum is heterogeneous given that all TAG precursors rendered fragment ions corresponding to 2 or 3 isobaric species (Table 2). The analysis allowed the identification of 28 different molecular TAG species. To our knowledge, this is the first report documenting the FA composition of TAG species in mouse brain tissue.

Molecular profiling of Cer species in adipocytes

Next, we tested the performance of the LC–MS workflow for charting Cer species in 3T3-L1 adipocytes. On differentiation to adipocytes, 3T3-L1 cells accumulate a large amount of TAGs, which decreases the amount of Cer relative to TAG and hampers the

analysis of Cer species. To optimize the detection of Cer species, we performed the LC–FTMS and LC–ITMS^2 workflow in negative ion mode so as to minimize TAG ionization and promote detection of Cer species. By executing the LC–FTMS procedure, we were able to identify 7 Cer species and profile them by normalizing the intensity of individual Cer species to the sum of intensities for all monitored Cer species (Table 3 and Fig 4B). The most abundant species was Cer 34:1;2, representing approximately 40% of all Cer species in both 3T3-L1 preadipocytes and adipocytes. No pronounced differences in the Cer profile between 3T3-L1 preadipocytes and adipocytes were observed (Fig. 4B). Subsequently, we reanalyzed the samples using the targeted LC–ITMS^2 routine so as to determine the FA composition of monitored Cer species. During the development of the LC–ITMS^2 procedure, we tested various instrumental settings for optimal detection of Cer-derived fragment ions. Surprisingly, we found that optimal detection of Cer-derived fragment ions was obtained by ITMS^2 of the precursor ion corresponding to $[Cer–H]^-$ and not the more abundant $[Cer+HCOO]^-$ adduct ion as detected by FTMS. We believe that this discrepancy is attributed to the "high-resolution ion isolation" that the IT instrumentation applies when using an ion isolation width below 2.0 amu. During ion isolation and fragmentation, the IT first ejects ions having higher m/z than the specified precursor m/z, followed by ejecting ions having lower m/z and subsequent ion activation. It appears that high-resolution ion isolation activates the $[Cer+HCOO]^-$ ion during isolation and promotes its dissociation to $[Cer–H]^-$, which is subsequently ejected prior to fragmentation and mass analysis. Conversely, when isolating the precursor corresponding to $[Cer–H]^-$, the $[Cer+HCOO]^-$ also becomes activated and dissociates to form $[Cer–H]^-$, which is subsequently available for ion activation and ITMS^2 analysis. Hence, to optimize the structural analysis of Cer species, we chose to target the precursor m/z corresponding to $[Cer–H]^-$.

The targeted LC–ITMS^2 analysis of Cer species showed structure-specific fragment ions corresponding to both the FA and LCB moiety that can be annotated as $[FA+C_2H_2NO_2]^-$ and $[LCB–H_5NO_2]^-$, respectively (Fig. 4C and Table 3). We note that these structure-specific fragment ions have been reported previously [28,29]. In summary, the analysis demonstrated that Cer species in 3T3-L1 preadipocytes and adipocytes comprise FA moieties ranging from 16 to 24 carbons (Table 3). These results corroborate previous observations reported for the Cer species profile of mouse adipose tissue [30]. Based on our results outlined above, we conclude that the integrated LC–FTMS and LC–ITMS^2 workflow is well suited for profiling low-abundant TAG and Cer species in complex sample matrices.

Conclusion

We have presented a novel lipidomics workflow based on normal-phase LC–FTMS and complementary LC–ITMS^2 for profiling and structural analysis of lipid species. The workflow uses a normal-phase LC system for separation of apolar and polar lipid species and uses a chip-based nanoelectrospray ion source and hybrid IT–orbitrap mass spectrometer for sensitive and specific lipid analysis. The workflow features a primary LC–FTMS survey routine for identification and profiling of lipid species based on high-mass accuracy and retention time and uses a targeted LC–ITMS^2 routine for identifying the FA moieties of monitored lipid species. We documented the performance of the workflow by in-depth analysis of low-abundant TAG species in mouse cerebellum and Cer species in adipocytes, two exceptionally challenging sample matrices. The presented lipidomics workflow is generic and can be extended to both comprehensive lipidome characterization and targeted analysis low-abundant lipid species.

Acknowledgments

We thank Kai Schuhmann and Wolfgang Metelmann-Strupat for expert advice on ITMS^2 analysis. We are grateful to Ole N. Jensen for kindly providing access to a TriVersa NanoMate ion source. We thank Nikolai Schmarowski for excellent technical assistance. This work was supported by Lundbeckfonden (R44-A4342), Danish Council for Strategic Research (11-116196) and the Danish Council for Independent Research | Natural Sciences (09-072484).

References

[1] A. Shevchenko, K. Simons, Lipidomics: coming to grips with lipid diversity, Nat. Rev. Mol. Cell. Biol. 11 (2010) 593–598.
[2] G. van Meer, Cellular lipidomics, EMBO J. 24 (2005) 3159–3165.
[3] M.P. Wymann, R. Schneiter, Lipid signalling in disease, Nat. Rev. Mol. Cell. Biol. 9 (2008) 162–176.
[4] X. Han, K. Yang, R.W. Gross, Multi-dimensional mass spectrometry-based shotgun lipidomics and novel strategies for lipidomic analyses, Mass Spectrom. Rev. 31 (2012) 134–178.
[5] R. Harkewicz, E.A. Dennis, Applications of mass spectrometry to lipids and membranes, Annu. Rev. Biochem. 80 (2011) 301–325.
[6] S.J. Blanksby, T.W. Mitchell, Advances in mass spectrometry for lipidomics, Annu. Rev. Anal. Chem. 3 (2010) 433–465.
[7] M.R. Wenk, The emerging field of lipidomics, Nat. Rev. Drug Discov. 4 (2005) 594–610.
[8] C.N. Serhan, Mediator lipidomics, Prostaglandins Other Lipid Mediat. 77 (2005) 4–14.
[9] M.C. Sullards, Y. Liu, Y. Chen, A.H. Merrill Jr., Analysis of mammalian sphingolipids by liquid chromatography tandem mass spectrometry (LC–MS/MS) and tissue imaging mass spectrometry (TIMS), Biochim. Biophys. Acta 2011 (1811) 838–853.
[10] B. Brugger, G. Erben, R. Sandhoff, F.T. Wieland, W.D. Lehmann, Quantitative analysis of biological membrane lipids at the low picomole level by nano-electrospray ionization tandem mass spectrometry, Proc. Natl. Acad. Sci. USA 94 (1997) 2339–2344.
[11] C.S. Ejsing, E. Duchoslav, J. Sampaio, K. Simons, R. Bonner, C. Thiele, K. Ekroos, A. Shevchenko, Automated identification and quantification of glycerophospholipid molecular species by multiple precursor ion scanning, Anal. Chem. 78 (2006) 6202–6214.
[12] D. Schwudke, J.T. Hannich, V. Surendranath, V. Grimard, T. Moehring, L. Burton, T. Kurzchalia, A. Shevchenko, Top-down lipidomic screens by multivariate analysis of high-resolution survey mass spectra, Anal. Chem. 79 (2007) 4083–4093.
[13] C.S. Ejsing, J.L. Sampaio, V. Surendranath, E. Duchoslav, K. Ekroos, R.W. Klemm, K. Simons, A. Shevchenko, Global analysis of the yeast lipidome by quantitative shotgun mass spectrometry, Proc. Natl. Acad. Sci. USA 106 (2009) 2136–2141.
[14] M. Stahlman, C.S. Ejsing, K. Tarasov, J. Perman, J. Boren, K. Ekroos, High-throughput shotgun lipidomics by quadrupole time-of-flight mass spectrometry, J. Chromatogr. B 877 (2009) 2664–2672.
[15] D.S. Myers, P.T. Ivanova, S.B. Milne, H.A. Brown, Quantitative analysis of glycerophospholipids by LC–MS: acquisition, data handling, and interpretation, Biochim. Biophys. Acta 2011 (1811) 748–757.
[16] H. Ogiso, T. Suzuki, R. Taguchi, Development of a reverse-phase liquid chromatography electrospray ionization mass spectrometry method for lipidomics, improving detection of phosphatidic acid and phosphatidylserine, Anal. Biochem. 375 (2008) 124–131.
[17] C.A. Haynes, J.C. Allegood, K. Sims, E.W. Wang, M.C. Sullards, A.H. Merrill Jr., Quantitation of fatty acyl-coenzyme As in mammalian cells by liquid chromatography–electrospray ionization tandem mass spectrometry, J. Lipid Res. 49 (2008) 1113–1125.
[18] M. Hermansson, A. Uphoff, R. Kakela, P. Somerharju, Automated quantitative analysis of complex lipidomes by liquid chromatography/mass spectrometry, Anal. Chem. 77 (2005) 2166–2175.
[19] U. Sommer, H. Herscovitz, F.K. Welty, C.E. Costello, LC–MS-based method for the qualitative and quantitative analysis of complex lipid mixtures, J. Lipid Res. 47 (2006) 804–814.
[20] J.F. Brouwers, Liquid chromatographic–mass spectrometric analysis of phospholipids: chromatography, ionization, and quantification, Biochim. Biophys. Acta 2011 (1811) 763–775.
[21] D.G. McLaren, P.L. Miller, M.E. Lassman, J.M. Castro-Perez, B.K. Hubbard, T.P. Roddy, An ultraperformance liquid chromatography method for the normal-phase separation of lipids, Anal. Biochem. 414 (2011) 266–272.
[22] J.L. Sampaio, M.J. Gerl, C. Klose, C.S. Ejsing, H. Beug, K. Simons, A. Shevchenko, Membrane lipidome of an epithelial cell line, Proc. Natl. Acad. Sci. USA 108 (2011) 1903–1907.
[23] F.S. Deschamps, P. Chaminade, D. Ferrier, A. Baillet, Assessment of the retention properties of poly(vinyl alcohol) stationary phase for lipid class profiling in liquid chromatography, J. Chromatogr. A 928 (2001) 127–137.
[24] M. Benghezal, C. Roubaty, V. Veepuri, J. Knudsen, A. Conzelmann, SLC1 and SLC4 encode partially redundant acyl-coenzyme A 1-acylglycerol-3-phosphate *O*-acyltransferases of budding yeast, J. Biol. Chem. 282 (2007) 30845–30855.

[25] K.L. Duffin, J.D. Henion, J.J. Shieh, Electrospray and tandem mass spectrometric characterization of acylglycerol mixtures that are dissolved in nonpolar solvents, Anal. Chem. 63 (1991) 1781–1788.
[26] A.M. McAnoy, C.C. Wu, R.C. Murphy, Direct qualitative analysis of triacylglycerols by electrospray mass spectrometry using a linear ion trap, J. Am. Soc. Mass Spectrom. 16 (2005) 1498–1509.
[27] D. Schwudke, J. Oegema, L. Burton, E. Entchev, J.T. Hannich, C.S. Ejsing, T. Kurzchalia, A. Shevchenko, Lipid profiling by multiple precursor and neutral loss scanning driven by the data-dependent acquisition, Anal. Chem. 78 (2006) 585–595.
[28] X. Han, Characterization and direct quantitation of ceramide molecular species from lipid extracts of biological samples by electrospray ionization tandem mass spectrometry, Anal. Biochem. 302 (2002) 199–212.
[29] F.F. Hsu, J. Turk, Characterization of ceramides by low energy collisional-activated dissociation tandem mass spectrometry with negative-ion electrospray ionization, J. Am. Soc. Mass Spectrom. 13 (2002) 558–570.
[30] F. Samad, K.D. Hester, G. Yang, Y.A. Hannun, J. Bielawski, Altered adipose and plasma sphingolipid metabolism in obesity: a potential mechanism for cardiovascular and metabolic risk, Diabetes 55 (2006) 2579–2587.